https://doi.org/10.36785/BUITEMS.JAES.316

Synthesis and Characterization of Lead Free Calcium Bismuth Titanate ($Ca_{0.25}Bi_{0.5}TiO_3$) Piezoelectric Ceramics

Alla ud Din[1], Asfandiyar[1], Fazal Wahid[1], Muhammad Rahim[2]*, Luqman I. Alrawi[3], Nadir Khan[1], Abdullah[1], Gohar Nqash[1], Arifullah Shah[1], Fazal Dad[1]

1-Department of Chemistry, Government College Peshawar, Khyber Pakhtunkhwa, Pakistan
2-School of Chemical Sciences, Universiti Sains Malaysia, 11800 Pulau Penang, Malaysia
3-Chemistry Department, College of Sciences, Kirkuk University, Kirkuk Iraq

Corresponding Author: kpk566@gmail.com

***Abstract*-- Bismuth layer-structured piezoelectric (BLSP) calcium bismuth titanate ($Ca_{0.25}Bi_{0.5}TiO_3$) piezoelectric ceramics have been prepared via a conventional sol gel reaction method by mixing the desired chemicals in stoichiometric amounts. Calcium bismuth titanate (CBT) samples were characterized by means of XRD, SEM and FTIR spectroscopy. X-ray diffraction (XRD) analysis revealed that CBT ceramics exhibit a single phase orthorhombic structure. The SEM images confirm its morphological size ranging from 1.00 to 2.75 µm. FTIR analysis reveals that calcium bismuth titanate has been prepared successfully, and the ratio of calcium, bismuth and titania was found to be 0.25:0.50:1.00, respectively. The photocatalytic removal of Methylene Blue, cadmium (Cd^{2+}) and other toxic heavy metals will be carried out using CBT materials.**

***Keywords*- Calcium Bismuth Titanate, Piezoelectric ceramic, Sol gel**

Date Received 25-09-2019
Date Accepted 25-12-2019
Date Published 31-12-2019

I. INTRODUCTION

THE $PbZrO_3$–$PbTiO_3$ based ceramics are the most widely used piezoelectric materials, due to their superior properties. Whereas, lead based ceramics are highly toxic and cause environmental and human health hazards. Therefore, lead-free piezoelectric materials are of great interest due to their environment friendliness [1]. Such materials are attracting the attention of research scholars because of their possible usage in cars, sound generators and solar cells. Therefore, it is very necessary to synthesize lead-free piezoelectric ceramics with excellent electrical properties [2]. As such, there is a common method to enhance the properties of piezoelectric materials which is to introduce electron donor atoms. By this way, the activation energy may be enhanced due to lack of charge carriers. On the other hand, some acceptor ions with variable valences should be imported in order to trap loosely bond electrons in order to minimize leakage, and increase resistivity [3].

The function of the piezoelectric materials can be increased by substitution of B-site of Ti^{4+} by Co^{2+} ion. The cation presents at the center of oxygen octahedral structure may play a major structural role in the polarization process which might be due to slight change in B-site of the cationic radius [4]. Many researchers have worked to overcome these problems and improve their piezoelectric properties [5,6]. Bismuth sodium titanate ($Bi_{0.5}Na_{0.5}TiO_3$) was discovered by Smolensky in 1960 [7]. Bismuth sodium titanate (BNT) is very significant lead-free piezoelectric material which has perovskite crystal structure and strong ferroelectric properties. BNT has very large remanent polarization (Pr) and coercive field (Ec) at room temperature [8,9].

In addition, BNT is a very important precursor for lead-free piezoelectric ceramics with excellent electrical properties. Researchers are working to improve the properties of BNT based piezoelectric ceramics [10]. Takenaka *et al.* (1997) further reported relatively low dielectric constant and high electromechanical properties for $Bi_{0.5}Na_{0.5}TiO_3$ and $Bi_{0.5}K_{0.5}TiO_3$ systems. Yu *et al.* (2000) reported that $BaTi_{0.95}Zr_{0.05}O_3$ ceramics showed fairly satisfactory piezoelectric response. The BLSFs show comparatively low aging rate, low dielectric constant, low temperature coefficient of resonant frequency and very strong anisotropic electromechanical coupling factors [11]. The study was

conducted to find out formulation ratio of calcium and bismuth with titania. In this study calcium bismuth titanate was synthesized and characterized by means of various techniques.

II. MATERIAL AND METHODS

A. Materials

Calcium Bismuth Titanate (CBT) was synthesized by sol gel method. Calcium acetate 99.0 % (CAS: 62-54-4), bismuth nitrate 99.9 % (CAS: 1304-85-4), titanium dioxide 99.9 % (CAS: 13463-67-7) were used as raw materials. Whereas, stearic acid was used as a precursor. All the chemicals are analytical grade and purchased from sigma Aldrich.

B. Synthesis of CBT

Sol gel method was adopted to synthesize CBT. Calcium acetate of 0.713 g, 1.420 g of bismuth nitrate and 2.839 g of titanium oxide were added to 3.000 g of stearic acid. Stearic acid was used as reaction medium. The mixture was heated on a hot plate upto 50 °C tell the appearance of yellowish mass (gel). The gel was calcined at 800 °C for 2 hours. Stearic acid was removed during calcinations [12]. The color of the product was appeared as off-white.

C. Characterization

The dry powders form of the CBT materials was subjected to Rietveld-XRD analysis for evaluation of their structure. The phase composition of the CBT materials was determined using an X-ray diffractometer (JDX-3532). Scans were taken at *2θ values* ranging from 5° to 80°. Whereas, the crystallites size was determined from Debye-Scherrer equation of the X-ray diffraction pattern [13].

$$D = \frac{k\lambda}{\beta \cos\theta} \qquad (1)$$

where λ is the radiation wavelength (1.54 Å), *k* is the shape factor = 0.9, β is the full width of a diffraction line at one half of maximum intensity in radian. Morphological investigations of the CBT materials were carried out using Scanning Electron Microscope (JSM5910, JEOL, Japan). The samples were dried and coated onto gold film, and observed in the microscope under reduced pressure. The FT-IR spectrum of CBT materials was obtained using Perkin Elmer Spotlight-200 instrument. In addition, the Attenuated Total Reflection (ATR) technique was used to obtain the spectra. The background spectrum was collected before scanning the samples. The samples were scanned from 450 to 4500 cm^{-1}. Scanning resolution and number of scans were adjusted 4 cm^{-1} and 16, respectively.

III. RESULTS AND DISCUSSIONS

The X-rays diffraction analysis is an effective tool for determining the crystallite size and phase composition of materials. XRD analysis refer to the diffraction effects caused when electromagnetic radiations (X-ray) impact on crystal lattice of spacing *d* at an angle *θ* to the incident radiation beam. Wavelength λ of the incident beam interacts with the atoms of the crystalline material, in the result, atoms of the target materials start to oscillate with the same frequency. The reflected beam to be directed with an angle of 2*θ* to the transmitted beam [14,15].

The XRD pattern of the synthesized CBT at 2*θ* values ranging from 5°–80° is shown in Figure 1. The Miller indices of the XRD data are shown in Table 1. The XRD data of the CBT samples calcined at 800 ^{o}C showed quite sharper peaks indicating good crystallinity. In addition, the crystallite size and phase compositions are significantly affected.

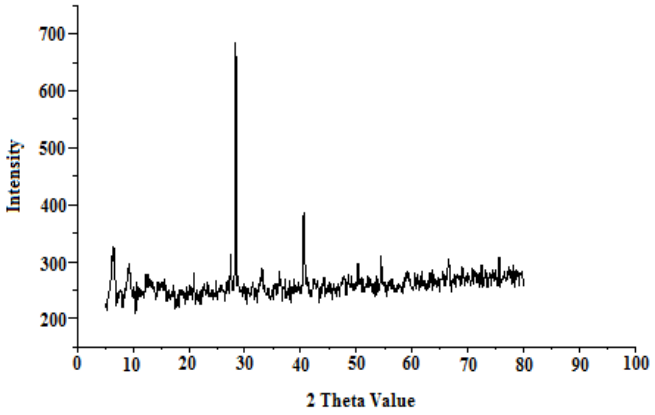

Fig. 1. XRD pattern of the CBT sample

TABLE 1
Miller indices of the XRD spectrum

2θ	h	k	I	Intensity(%)
27.45	1	1	7	313
37.20	1	0	15	265
38.80	1	2	5	268
40.60	1	1	15	386
44.20	0	0	20	267
49.15	2	0	16	222
50.20	2	2	8	297
53.60	3	1	1	275
54.30	2	2	12	301
55.90	3	1	7	238
66.4	1	1	27	305
69.15	3	0	29	273
69.15	3	2	13	268

A. Scanning Electron Microscopy (SEM) Analysis

The SEM image of CBT sample calcined at 800 °C is shown in the Figure 2. The image clearly shows that the CBT gained spheroid shape ranging from 1.00 to 2.75 µm. As such, doping process of metals increases surface roughness. Similarly, loosely bounded spheroid particles are restricted in more agglomerated manners. Choi *et al.* (2009) reported that doping of metals increases aggregation of particles and roughness of the surfaces [16]. Previous findings also showed that the doping TiO_2 with silver increased its aggregation [17,18].

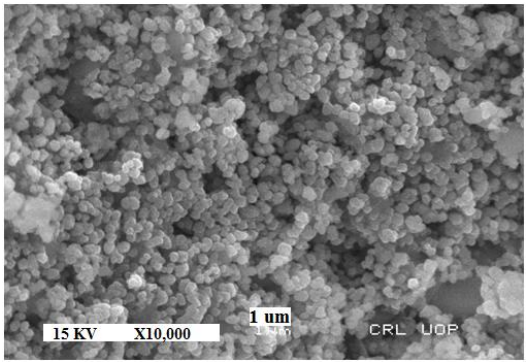

Fig. 2. Scanning Electron Micrograph (SEM) of CBT sample

B. Particle Size Distribution of CBT

The particles size distribution of CBT samples are shown in Figure 3. The maximum size of the particles were found to be 2.75 µm while the minimum size was observed as 1.00 µm. Whereas, the average particle size was found to be 1.60 µm, as shown in Table 2.

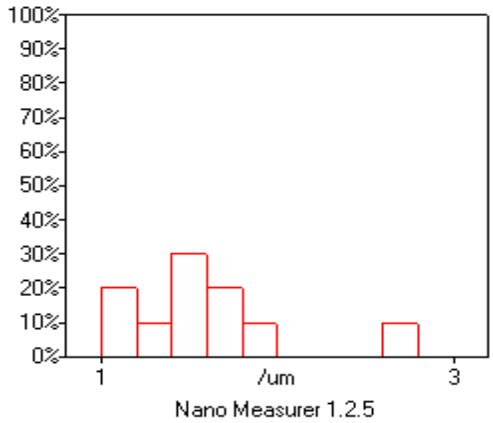

Fig. 3. Particle size distribution of the CBT

Table 2
Particle size distribution of CBT

Max. (Size)	2.75 (µm)
Min. (Size)	1.00 (µm)
Mean (Size)	1.60 (µm)
No.	Particle Size (µm)
1	1.87
2	1.47
3	1.54
4	2.75
5	1.76
6	1.54
7	1.00
8	1.76
9	1.32
10	1.01

C. Fourier Transform Infrared Spectra

Rahimi *et al*., (2015) reported that the broad intense peak lower than 700 cm^{-1} corresponding to Ti-O-Ti vibration bands [19]. Rahim *et al*., (2016) reported that the weak absorption bands at 1620-1635 cm^{-1} and 3350-3450 cm^{-1} correspond to the bending and stretching vibrations of O−H, respectively [20]. According to Hamadaian *et al.* (2009), the intensity of O−H bending and stretching vibrations decreases with the increase in calcination temperature which indicate removal of absorbed water molecules [21].

The FT-IR spectrum of the CBT materials is shown in Figure 4. A well defined absorption band at around 1094 cm^{-1}, and one broad band in the range 520 cm^{-1} to 541 cm^{-1} were observed in the spectrum of CBT samples. The Broad absorption band at around 520 cm^{-1} to 541 cm^{-1} has been assigned to the stretching vibration Ti-O. Whereas, weak absorption band at 403 cm^{-1} to 415cm^{-1}corresponds to the bending vibration of Ti-O [16].

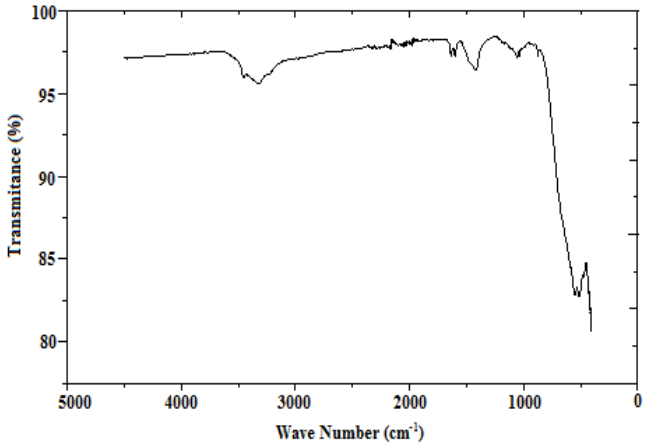

Fig. 4. Fourier Transform Infrared (FTIR) Spectra for CBT

IV. CONCLUSIONS

The piezoelectric ceramic materials $Ca_{0.25}Bi_{0.5}TiO_3$ (CBT) was synthesized successfully by sol-gel method. Samples were characterized by the XRD, SEM and FT-IR techniques. XRD analysis confirmed that CBT exhibit a single phase orthorhombic structure with an irregular morphology. The formulation ratio of calcium and bismuth with titanium was found to be 0.25:0.50:1.00 respectively. SEM images confirm the CBT layered structure sizing from 1.00 µm to 2.75 µm. FT-IR analysis indicated an absorption band at around 1094 cm^{-1}, and one broad band in the range of 520 cm^{-1} to 541 cm^{-1} were observed in the spectra of CBT materials. The Broad absorption band at around 521 cm^{-1} to 541 cm^{-1} is assigned to Ti–O stretching vibration and weak absorption band at 403 cm^{-1} to 415cm^{-1} was assigned to the Ti–O bending vibration [16]. The FT-IR spectrum confirms the chemical combination of calcium and bismuth with the titania.

The photocatalytic removal of Methylene Blue, cadmium (Cd^{2+}) and other toxic heavy metals will be carried out using CBT materials by our research group.

V. ACKNOWLEDGMENT

The authors acknowledge the financial support of National Center of Excellence, University of Peshawar. The facilitating support of Centralized Resource Laboratory and Material Testing Laboratory, Department of Physics, University of Peshawar (Pakistan), is highly acknowledged.

VI. REFERENCES

[1] T. Ibn-Mohammed, S. C. L. Koh, I. M. Reaney, D. C. Sinclair, K. B. Mustapha, A. Acquaye and D. Wang. (2017). Are lead-free piezoelectrics more environmentally friendly. *MRS Communications.* 7(1), pp. 1–7.

[2] Z. Y. Shen, H. Sun, Y. Tang, Y. Zhang and S. Li. (2015). Enhanced piezoelectric properties and excellent thermal stabilities of cobalt-modified Aurivillius-type calcium bismuth titan ate ($CaBi_4Ti_4O_{15}$). *Materials ResearchBulletin*. 63, pp. 129–133.

[3] H. Chen, B. Shen, J. Xu and J. Zhai. (2013).The grain size-dependent electrical properties of Bi4Ti3O12 piezoelectric ceramics. *Journal of Alloys and Compounds*. 551, pp. 92–97.

[4] A. Tanwar, M. Verma, V. Gupta and K. Sreenivas. (2011). A-site substitution effect of strontium on bismuth layered $CaBi_4Ti_4O_{15}$ ceramics on electrical and piezoelectric properties. *Material Chemistry and Physics*. 130(1-2), pp. 95–103.

[5] X. Wang, C. He and X. Fu. (2014). Electrical performance and microstructure of Li and Mn co-doped Aurivillius-type. *Journal of Materials Sciences*. 25, pp. 3396–3402.

[6] G. A. Smolensky, V. A. Isopov and J. Argranovskaya. (1961). Structural and dielectric behavior of doped bismuth sodium titanate: Lead free piezoelectric materials. *Solid State Physics*. 2, pp. NN.

[7] H. Yan, Z. Zhang, W. Zhu, L. He, Y. Yu and C. Li. (2004). Lead free piezoelectric. *Materials Research Bulletin*. 39, pp. 1237–1246.

[8] X. Wang, X. G. Tang, H. L. W. Chan and P. K. Choy. (2005). Solid State Community. 134, pp. 659–663.

[9] X. Wang, H. L.W. Chan and C. L. Choy. (2003). Synthesis and characterization of piezoelectric. *Solid State Community*. 125, pp. 395–399.

[10] T. Takenaka, T. Okuda and K. Takegahara. (1997). Dielectric behavior and microstructure of $(Bi_{0.5}Na_{0.5})$ TiO_3BaTiO_3 lead-free piezoelectric ceramics. *Ferroelectrics*. 196, pp. 175–178.

[11] Z. Yu, R. Y. Guo and A. S. Bhalla. (2000). Structure and electrical properties of 001 textured $(Ba_{0.85}Ca_{0.15})(Ti_{0.9}Zr_{0.1})O_3$ lead-free piezoelectric ceramics. *Applied Physics Letter*. 77, pp. 15–35.

[12] S. Kawamori and T. Machida. (2008). Silicon carbide dispersion strengthening of magnesium using mechanical alloying method. Materials Transactions. 49, pp. 304-309.

[13] G. Liu, D. Zhu, S. Liao, L. Ren, J. Cui and W. Zhou. (2009). Solid-phase photocatalytic degradation of polyethylene–goethite composite film under UV-light irradiation. *Journal of hazardous materials*.172(2), pp. 1424–1429.

[14] L. I. Halaoui, N. M. Abrams and T. E. Mallouk. (2005). Increasing the conversion efficiency of dye-sensitized TiO_2 photoelectrochemical cells by coupling to photonic crystals. *The Journal of Physical Chemistry B.* 109(13), pp. 6334–6342.

[15] C. Hammond and C. Hammond. (2009). The basics of crystallography and diffraction (Vol. 12): Oxford University Press Oxford.

[16] J. Choi, H. Park and M. R. Hoffmann. (2009). Effects of single metal-ion doping on the visible-light photoreactivity of TiO_2. *The Journal of Physical Chemistry C*. 114(2), pp. 783–792.

[17] C. C. Chang, C. K. Lin, C.C. Chan, C. S. Hsu and C. Y. Chen. (2006). Photocatalytic properties of nanocrystalline TiO_2 thin film with Ag additions. *Thin Solid Films*. 494(1), pp. 274–278.

[18] R. Liu, H. Wu, R. Yeh, C. Lee and Y. Hung. (2012). Synthesis and bactericidal ability of TiO_2 and Ag-TiO_2 prepared by coprecipitation method. *International Journal of Photoenergy*. 6, pp. 46–51.

[19] R. Rahimi, S. Zargari, A. Ghaffarinejad and A. Morsali. (2015). Investigation of the synergistic effect of porphyrin photosensitizer on graphene–TiO_2 nanocomposite for visible light photoactivity improvement. *Environmental Progress & Sustainable Energy*. 65, pp. 78–84.

[20] M. Rahim, N. Abu and M. R. H. Mas Haris. (2016). The effect of pH on the slow-release behaviour of 1- and 2-naphthol from chitosan film. *Cogent Chemistry*. 2, pp.1234345.

[21] M. Hamadanian, A. Reisi-Vanani and A. Majedi. (2009). Preparation and characterization of S-doped TiO_2NPs, effect of calcination temperature and evaluation of photocatalytic activity. *Materials Chemistry and Physics*.116(2), pp. 376–382.